The Regulation of Vascular Endothelial Growth Factor-induced Microvascular Permeability Requires Rac and Reactive Oxygen Species*

Elizabeth Monaghan-Benson[1] **and Keith Burridge**

From the Department of Cell and Developmental Biology and Lineberger Cancer Center, University of North Carolina, Chapel Hill, North Carolina 27599

Vascular permeability is a complex process involving the coordinated regulation of multiple signaling pathways in the endothelial cell. It has long been documented that vascular endothelial growth factor (VEGF) greatly enhances microvascular permeability; however, the molecular mechanisms controlling VEGF-induced permeability remain unknown. Treatment of microvascular endothelial cells with VEGF led to an increase in reactive oxygen species (ROS) production. ROS are required for VEGF-induced permeability as treatment with the free radical scavenger, *N*-acetylcysteine, inhibited this effect. Additionally, treatment with VEGF caused ROS-dependent tyrosine phosphorylation of both vascular-endothelial (VE)-cadherin and β-catenin. Rac1 was required for the VEGF-induced increase in permeability and adherens junction protein phosphorylation. Knockdown of Rac1 inhibited VEGF-induced ROS production consistent with Rac lying upstream of ROS in this pathway. Collectively, these data suggest that VEGF leads to a Rac-mediated generation of ROS, which, in turn, elevates the tyrosine phosphorylation of VE-cadherin and β-catenin, ultimately regulating adherens junction integrity.

Endothelial cells line the inside of blood vessels and serve as a barrier between circulating blood and the surrounding tissues. Endothelial permeability is mediated by two pathways: the transcellular pathway and the paracellular pathway. In the transcellular pathway material passes through the cells, whereas in the paracellular pathway fluid and macromolecules pass between the cells. The paracellular pathway is regulated by the properties of endothelial cell-cell junctions (1–3). Changes in the permeability of this barrier are tightly regulated under normal physiological conditions. However, dysregulated vascular permeability is observed in many life-threatening conditions, including heart disease, cancer, stroke, and diabetes.

VEGF[2] was first discovered as a potent vascular permeability factor that stimulated a rapid and reversible increase in micro-vascular permeability without damaging the endothelial cell (4, 5). VEGF was later shown to be a selective growth factor for endothelial cells, capable of promoting migration, growth, and survival (6). Considerable progress has been made toward understanding the signaling events by which VEGF promotes growth and survival (7). However, the mechanism through which VEGF promotes microvascular permeability remains incompletely understood.

VE-cadherin is an endothelial cell-specific adhesion molecule that connects adjacent endothelial cells (8, 9). While the barrier function of the endothelium is supported by multiple cell-cell adhesion systems, disruption of VE-cadherin is sufficient to disrupt intercellular junctions (9–11). Earlier studies have demonstrated increased permeability both *in vitro* and *in vivo* after treatment with VE-cadherin-blocking antibodies (9, 12). Additionally, VE-cadherin is required to prevent disassembly of blood vessel walls (11, 13) and to coordinate the passage of macromolecules through the endothelium (14, 15). Tyrosine phosphorylation may provide the regulatory link, as increased phosphorylation of cadherins and potential dissociation of the cadherin/catenin complex results in decreased cell-cell adhesion and increased permeability (16, 17).

Recent evidence has demonstrated that Rac1-induced reactive oxygen species (ROS) disrupt VE-cadherin based cell-cell adhesion (18). The mechanisms by which ROS affect endothelial permeability have not been fully characterized. VEGF has been reported to induce NADPH oxidase activity and induce the formation of ROS (19, 20). A direct link between Rac and ROS in a non-phagocytic cell was shown in 1996, when it was demonstrated that activated Rac1 resulted in the increased generation of ROS in fibroblasts (21). Several studies have subsequently implicated Rac-mediated production of ROS in a variety of cellular responses, in particular in endothelial cells (22, 23). These data suggest that ROS may play a critical role in integrating signals from VEGF and Rac to regulate the phosphorylation of VE-cadherin and ultimately the integrity of the endothelial barrier.

In the present study we sought to determine the mechanism by which VEGF regulates microvascular permeability. Our results show that VEGF treatment of human microvascular endothelial cells results in the Rac-dependent produc-

[2] The abbreviations used are: VEGF, vascular endothelial growth factor; ROS, reactive oxygen species; PTP, protein-tyrosine phosphatase; VE-cadherin, vascular-endothelial cadherin; GFP, green fluorescent protein; DCF, 6-car-boxy-2′,7′-dichlorofluorescein diacetate di(acetoxymethyl ester); HMVEC, human pulmonary microvessel endothelial cell; WT, wild type; siRNA, small interference RNA; FITC, fluorescence isothiocyanate; NAC, *N*-acetylcysteine; DPI, diphenyleneiodonium chloride; PAK, p21-activating kinase.

tion of ROS and the subsequent tyrosine phosphorylation of VE-cadherin and β-catenin. The phosphorylation of VE-cadherin and β-catenin are dependent on Rac and ROS and result in decreased junctional integrity and enhanced vascular permeability.

EXPERIMENTAL PROCEDURES

Reagents and Antibodies—Unless otherwise stated all chemicals were obtained from Sigma. DCF was obtained from Molecular Probes (Eugene, OR). Recombinant human VEGF$_{165}$ was purchased from R&D Systems (Minneapolis, MN). DPI was purchased from Calbiochem. The total VE-cadherin antibody and the p120 catenin antibody were obtained from Santa Cruz Biotechnology, and the phospho-specific VE-cadherin antibodies were from BIOSOURCE (Camarillo, CA). The antibody against Rac1 was from BD Biosciences. The β-catenin PY654 antibody was from AbCam. Monoclonal antibody to phosphotyrosine (clone 4G10) was obtained from Upstate Biotechnology.

Cell Culture—Human pulmonary microvessel endothelial cells (HMVECs) were obtained from Lonza and grown in Lonza's EGM-2-MV medium on collagen-coated (20 μg/ml) tissue culture dishes according to the manufacturer's instructions.

ROS Generation—Formation of ROS was monitored by the conversion of non-fluorescent 6-carboxy-2′,7′-dichlorodihydrofluorescein diacetate di(acetoxymethyl ester) to fluorescent DCF. Cells were loaded with 5 μM DCF in serum-free medium for 30 min at 37 °C. After loading, cells were washed twice with phosphate-buffered saline, and incubated for an additional 20 min at 37 °C to allow for dye de-esterification. Cells were stimulated as described in the figure legends. Fluorescence was determined using a fluorometer with an excitation of 485 and an emission of 520.

siRNA Transfection—Cells plated at ~50% confluence and left overnight were transfected with siRNA (Dharmacon) at a concentration of 25 nM using Oligofectamine (Invitrogen) according to the manufacturer's instructions. A non-targeting siRNA (Dharmacon) was used as a control. Cells were transfected for 4 h in serum-free medium, following which 1.5 ml of EGM-2MV was added. Cells were harvested after 72 h.

Adenoviral Infection of HMVECs—Wild-type VE-cadherin, VE-cadherin Y658F, VE-cadherin Y731F, and VE-cadherin Y658F/Y731F were generated as previously described (24). HMVECs were infected with adenovirus for 48 h in EGM-2MV. Infection efficiency (>85%) was monitored through the visualization of GFP, which is coexpressed by these recombinants.

FITC-Dextran Flux—HMVECs were grown to confluence for a minimum of 3 days in the top well of a Transwell filter (0.4 μM, 12-mm diameter, Corning). Cells were serum-starved for 2 h before treatment with VEGF. Treatment doses and times are as detailed in the figure legends. 10-kDa FITC-dextran (Molecular Probes) was added to the top chamber of the Transwell for a final concentration of 1 mg/ml. After 1 h, as sample was removed form the bottom compartment and read in a fluorometer (FluorStar Optima, BMG Labtech, excitation 485 nm, emission 520 nm).

Immunofluorescence and Microscopy—HMVECs were grown on collagen-coated coverslips. Cells were then treated with NAC for 2 h before treatment with 10 ng/ml VEGF for 15 min. After VEGF treatment cells were fixed for 15 min in 3% paraformaldehyde, permeabilized in 0.3% Triton X-100, and blocked for 30 min in 2% bovine serum albumin. To visualize VE-cadherin cells were stained with a monoclonal antibody against VE-cadherin (Santa Cruz Biotechnology) followed by goat anti-mouse Alexa 488 (Molecular Probes). Immunofluorescence images were taken with a Zeiss axiovert 200M microscope equipped with a Hamamatsu ORCA-ERAG digital camera and Metamorph workstation (Universal Imaging Corp.).

Rac1 Activity Assays—Cells were stimulated as indicated in the figure legends. After stimulation cells were kept on ice, washed with ice-cold phosphate-buffered saline, and assayed for Rac activation with glutathione *S*-transferase-p21-activating kinase, as described by Sander *et al.* (62). The beads were washed four times with lysis buffer, and after the final wash beads were resuspended in sample buffer. Samples were then analyzed by SDS-PAGE.

Immunoprecipitation and Immunoblotting—Cell layers were serum-starved for 2 h before stimulation with VEGF. Treatment doses and times are provided in the figure legends. For immunoprecipitation, cells were extracted on ice for 30 min in lysis buffer (10 mM Tris, pH 7.4, 150 mM NaCl, 1% Triton X-100, 0.5% Nonidet P-40, protease, and phosphatase inhibitors). After preclearing with protein A/G-agarose beads, lysates were incubated with antibodies to VE-cadherin, p120 catenin, or β-catenin for 2 h at 4 °C. After washing three times, the beads were resuspended in sample buffer, boiled for 10 min, and analyzed by Western blotting. For whole cell lysate analysis, cells were rinsed in phosphate-buffered saline and lysed in sample buffer. Lysates were electrophoresed into SDS-PAGE gels. Proteins were transferred to nitrocellulose membranes (Schleicher and Schuell Bioscience) and processed for Western analysis using the antibodies described in the figure legends. Bound antibodies were detected by enhanced chemiluminescence. For quantification of Western blots, intensity values of bands were measured from three different repeats for each experiment using ImageJ (National Institutes of Health).

RESULTS

To determine if VEGF treatment caused an increase in the production of ROS in HMVECs we directly monitored intracellular ROS formation, using the conversion of the non-fluorescent 6-carboxy-2′,7′-dichlorodihydrofluoroscein to DCF. As seen in Fig. 1*A*, treatment of HMVECs with increasing doses of VEGF stimulated a dose-dependent increase in ROS production as demonstrated by a net increase in cell fluorescence. H_2O_2, a known ROS, was used as a positive control. The time course of VEGF-induced ROS generation was then examined. ROS generation was observed as early as 5 min after treatment with VEGF (Fig. 1*B*). To confirm that the increase in DCF fluorescence observed upon VEGF treatment was due to an increase in ROS generation the free radical scavenger, NAC, was used. HMVECs were treated with increasing doses of NAC before treatment with VEGF. ROS generation was then measured by DCF fluorescence (Fig. 1*C*). As expected, treatment with NAC caused a dose-dependent decrease in DCF fluorescence confirming that the increase fluorescence was due to an
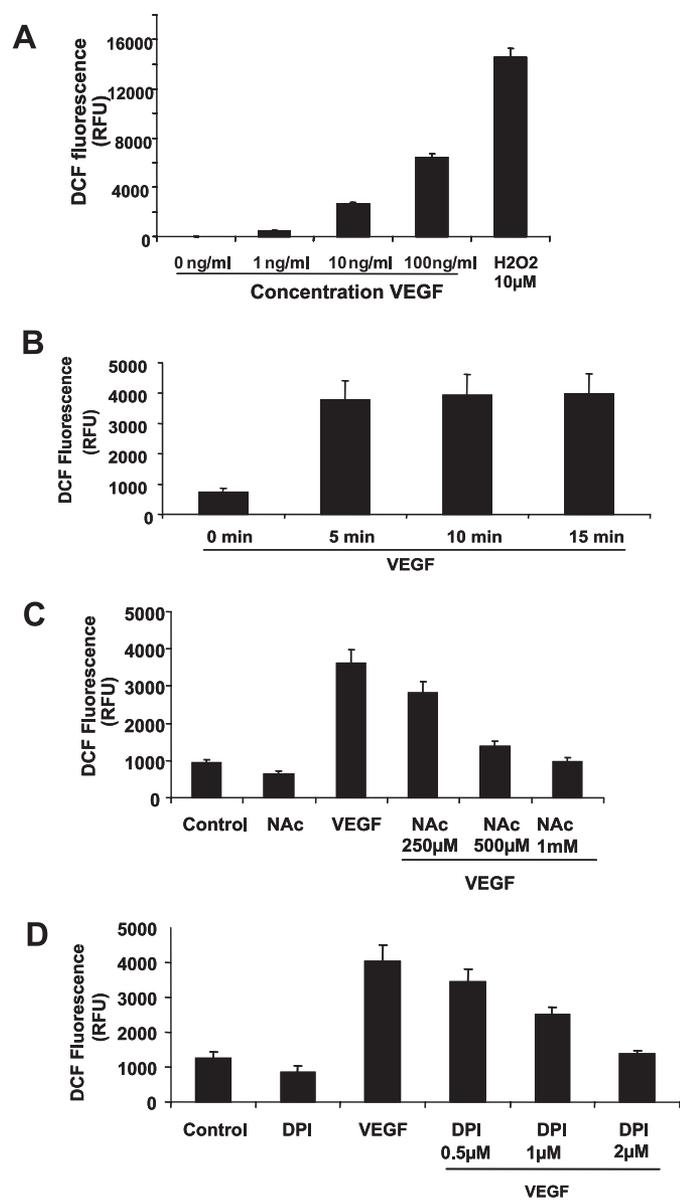
FIGURE 1. **VEGF treatment causes an increase in the generation of ROS.** *A*, confluent monolayers of HMVECs were loaded with DCF and then treated with increasing doses of VEGF for 15 min. The generation of ROS was measured by the fluorescence intensity of DCF. *B*, confluent monolayers of HMVECs were loaded with DCF and then treated with 10 ng/ml VEGF for 5, 10, and 15 min. The generation of ROS was measured by the fluorescence intensity of DCF. *C* and *D*, HMVECs were pretreated with NAC (*B*) or DPI (*C*) for 2 h. Cells were then loaded with DCF and treated with 10 ng/ml VEGF for 10 min. The generation of ROS was measured by the fluorescence intensity of DCF. These are representative graphs of an $n = 3$ performed in quadruplicate.

increase in ROS generation. In many cell types, including endothelial cells the major producer of ROS is NADPH oxidase (25). To determine if NADPH oxidase may be involved in VEGF-induced ROS production the flavoprotein inhibitor, DPI, was used to inhibit NADPH oxidase activity. Treatment with DPI caused a dose-dependent decrease in ROS production, suggesting that NADPH oxidase may be involved (Fig. 1*D*).

VEGF is a known, potent inducer of permeability in the microvasculature (4). We sought to determine if the VEGF-induced increase in microvascular permeability requires ROS, through the use of a FITC-dextran Transwell assay to measure

endothelial cell monolayer permeability. Endothelial cells grown to confluence on Transwell filters were stimulated with VEGF, resulting in an increase in the passage of FITC-dextran across the monolayers (Fig. 2*A*). However, this increase in permeability after VEGF treatment was attenuated by treatment with the ROS scavenger, NAC. Similar results were observed when cells were treated with DPI. Although VEGF caused an increase in microvascular permeability, treatment with DPI inhibited the VEGF-induced permeability increase (Fig. 2*B*). Vascular permeability is regulated, in part, by the integrity of junctions between neighboring endothelial cells. One of the major adhesion molecules that regulates the integrity of endothelial junctions is VE-cadherin. Therefore, we wanted to determine if any visible change was occurring in the localization of VE-cadherin after VEGF treatment (Fig. 2*C*). We found that under control conditions VE-cadherin staining is primarily seen as a tight line bordering the endothelial cells at the cell-cell junctions (Fig. 2*C*, *panel a*). However, upon VEGF treatment we found that VE-cadherin staining becomes much more jagged and that visible gaps are seen between neighboring endothelial cells (Fig. 2*C*, *panel c*). If ROS are scavenged with NAC we found that the VEGF-induced changes in VE-cadherin staining are attenuated (Fig. 2*C*, *panel d*). Taken together with Fig. 1 these data indicate that VEGF treatment leads to the production of ROS and that these ROS are required for the increase in microvascular permeability.

Tyrosine phosphorylation of various adherens junction molecules in the endothelium is indicative of decreased junctional integrity (26, 27). One of the major adhesion molecules of endothelial junctions is VE-cadherin. To determine if VEGF treatment caused any change in the tyrosine phosphorylation of VE-cadherin, VE-cadherin was immunoprecipitated and general phosphotyrosine levels were analyzed. As demonstrated in Fig. 3*A*, treatment with VEGF caused enhanced tyrosine phosphorylation of VE-cadherin in HMVECs. Phosphorylation of VE-cadherin at tyrosines 658 and 731 has been shown to inhibit the binding of p120-catenin and β-catenin, respectively (17). To investigate whether VEGF treatment has any effect on the catenin binding sites of VE-cadherin, HMVECs were treated with VEGF for increasing amounts of time and the phosphorylation at Tyr-658 and Tyr-731 were monitored. Treatment with VEGF caused enhanced phosphorylation of both of these residues on VE-cadherin as early as 5 min after treatment (Fig. 3*B*). To determine if ROS were required for these VEGF-induced effects on VE-cadherin tyrosine phosphorylation, NAC and DPI were again used (Fig. 3, *C* and *D*). In both cases we observed that VEGF was no longer able to cause phosphorylation of VE-cadherin after treatment with NAC or DPI, suggesting that ROS are required for phosphorylation of VE-cadherin at the catenin binding sites. Similar results were seen when β-catenin was examined. Immunoprecipitation analysis revealed enhanced tyrosine phosphorylation of β-catenin after VEGF treatment (Fig. 4*A*). Examination of Tyr-654 revealed elevated phosphorylation in response to VEGF (Fig. 4*B*) that was inhibited upon NAC treatment (Fig. 4*C*) and treatment with DPI (Fig. 4*D*).

To determine if the phosphorylation of VE-cadherin at tyrosines 658 and 731 was critical to the ability of VEGF to

A

B

C
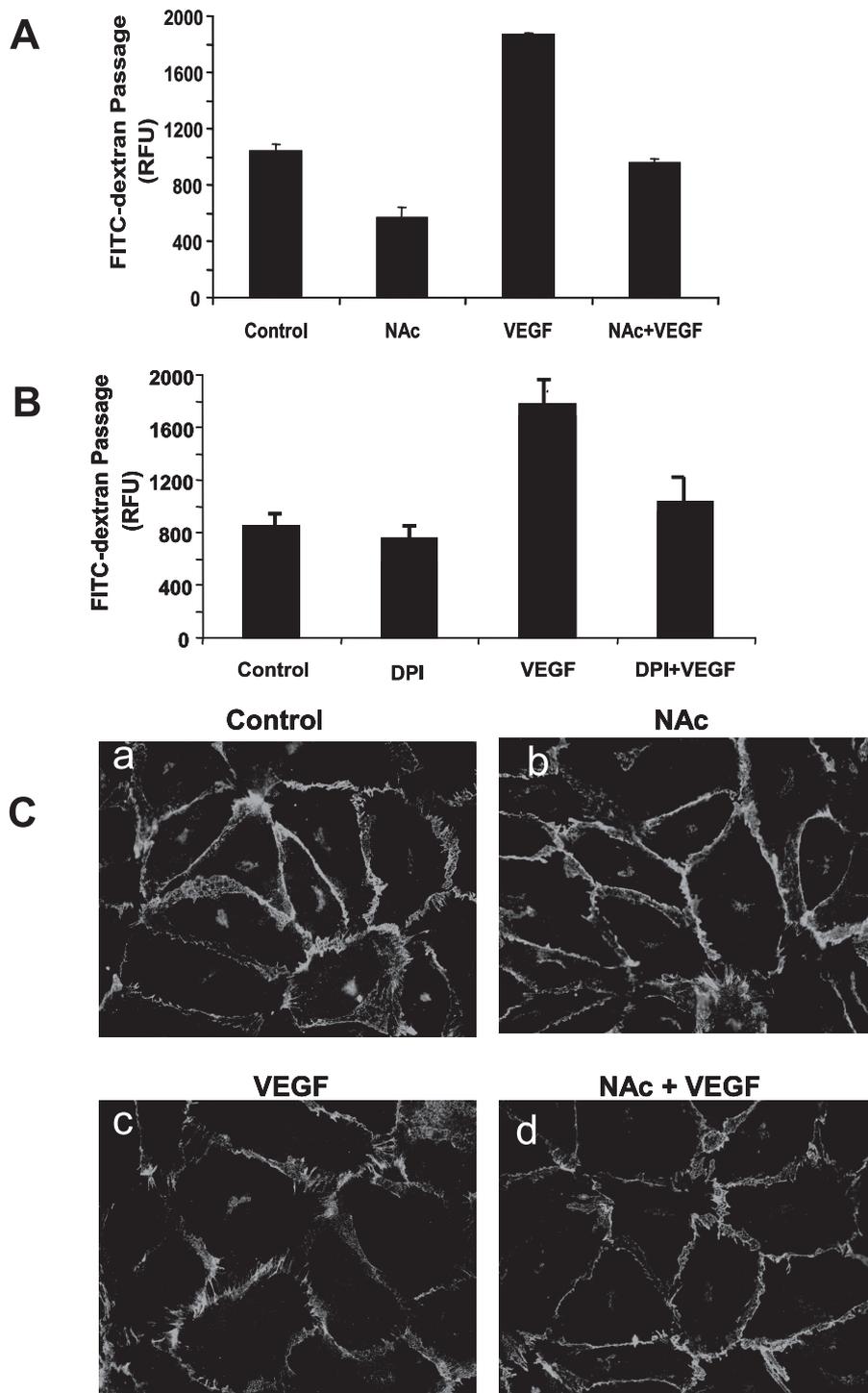
FIGURE 2. **VEGF induced permeability requires ROS.** HMVECs were seeded in the upper well of a Transwell chamber and allowed to grow to confluence. Cells were treated with NAC (*A*) or DPI (*B*) before 1 mg/ml FITC-dextran (M_r 10,000) was placed in the upper well, and cells were treated with 10 ng/ml VEGF for 30 min. A sample of medium from the lower chamber was then taken, and the amount of FITC-dextran in the lower chamber was measured in a plate reader. These are representative graphs of an *n* = 3 performed in quadruplicate. *C*, HMVECs were grown on coverslips and appropriate wells treated with NAC for 2 h before treatment with VEGF for 15 min. Cells were then fixed, permeabilized, and stained with an antibody against VE-cadherin. *Panel a*, control treated cells; *panel b*, NAC-treated cells; *panel c*, VEGF-treated cells; *panel d*, NAC/VEGF-treated cells.

mutated to phenylalanine (Y731F) or a double mutant where both tyrosines 658 and 731 had been mutated to phenylalanines (Y658F/Y731F) (Fig. 5*A*) (24). We first sought to determine if mutation at these tyrosine residues had any effect on the ability of VEGF to induce tyrosine phosphorylation of VE-cadherin. Under control conditions expression of any of the VE-cadherin viruses had no effect on basal phosphotyrosine levels (Fig. 5*B*). Upon stimulation with VEGF we find that there is enhanced tyrosine phosphorylation of VE-cadherin in cells infected with the WT virus. In cells infected with the Y658F or Y731F viruses there is a reduced level of tyrosine phosphorylation when compared with cells infected with WT. There is even a further reduction in VE-cadherin tyrosine phosphorylation when the Y658F/Y731F mutant was examined. To determine if these VE-cadherin tyrosine residues were critical to the ability of VEGF to enhance microvascular permeability, the HMVECs were infected with the VE-cadherin viruses and permeability was assessed through FITC-dextran flux (Fig. 5*C*). A GFP virus was used as a control. Under control conditions expression of any of the VE-cadherin viruses had no effect on basal vascular permeability. Upon VEGF treatment cells infected with GFP or WT VE-cadherin showed an increase in vascular permeability. Infection with either single VE-cadherin mutant (Y658F or Y731F) had little effect on the ability of VEGF to enhance vascular permeability. However, infection with the double mutant (Y658F/Y731F) significantly decreased the ability of VEGF to enhance permeability. To evaluate if phosphorylation at Tyr-658 and Tyr-731 was important in the regulation of VE-cadherin/catenin interactions, in response to VEGF treatment, we again utilized the VE-cadherin WT, Y658F, Y731F, and Y658F/Y731F adenoviral constructs. We first examined the relationship between VE-cadherin and p120-catenin by co-immunoprecipitation analysis. We found that in cells expressing WT VE-cadherin

induce enhanced vascular permeability, HMVECs were infected with adenovirus containing either wild-type VE-cadherin (WT), VE-cadherin in which Tyr-658 was mutated to phenylalanine (Y658F), VE-cadherin in which Tyr-731 was
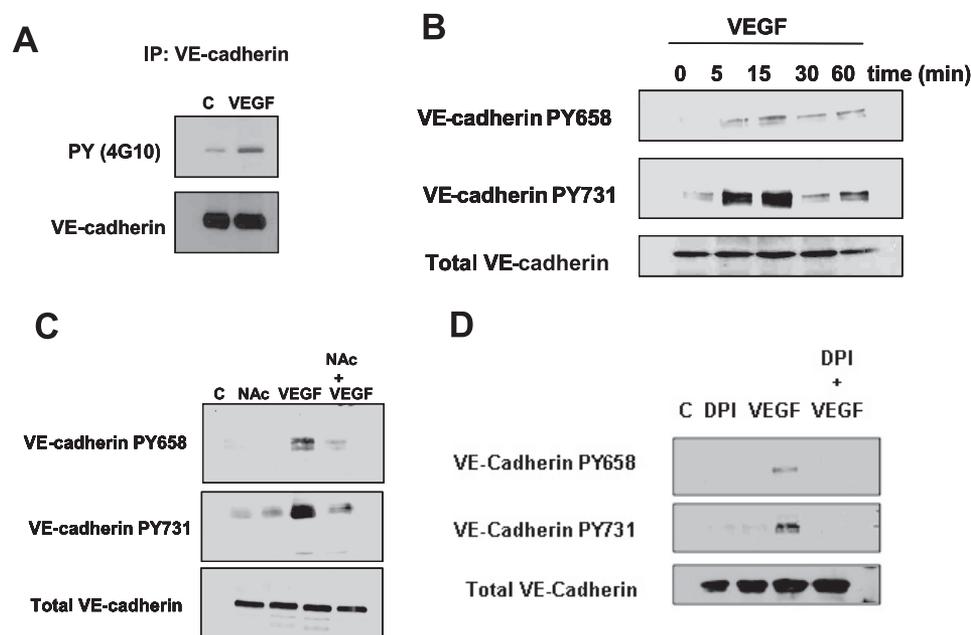
FIGURE 3. **VEGF treatment causes ROS-dependent phosphorylation of VE-cadherin.** Monolayers of HMVECs were treated with 10 ng/ml VEGF. *A*, VE-cadherin was immunoprecipitated from cell lysates using a mouse anti-VE-cadherin antibody, and the resulting immunoprecipitates were analyzed for phosphotyrosine by immunoblotting (4G10, *top*) or total VE-cadherin (*bottom*). *B*, cell layers were lysed in sample buffer. Lysates were electrophoresed, immunoblotted, and analyzed for phosphorylated forms of VE-cadherin using antibodies that specifically recognize VE-cadherin phosphorylated at tyrosines 658 and 731. Total VE-cadherin was used as a loading control. *C* and *D*, HMVECs were pretreated with NAC (*C*) or DPI (*D*) before treatment with 10 ng/ml VEGF, and the phosphorylation of VE-cadherin was monitored by Western blotting.
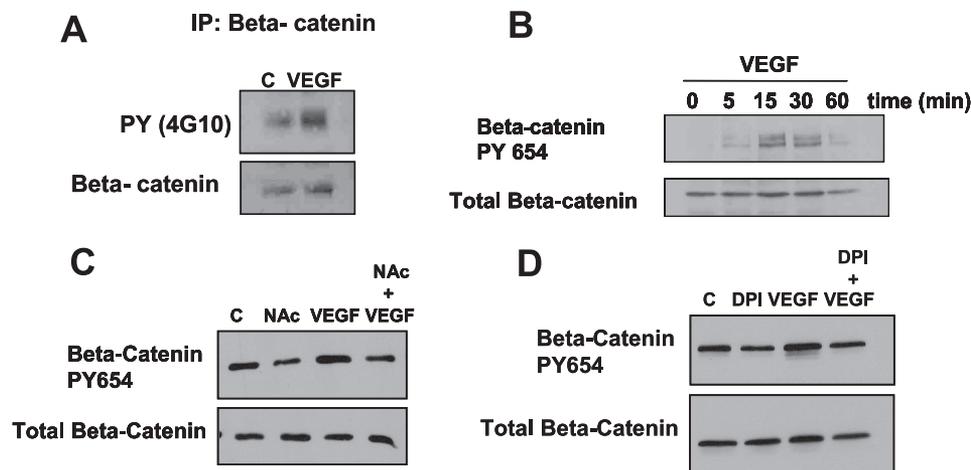
FIGURE 4. **VEGF treatment causes ROS-dependent phosphorylation of β-catenin.** Monolayers of HMVECs were treated with 10 ng/ml VEGF. *A*, β-catenin was immunoprecipitated from cell lysates using a mouse anti-β-catenin antibody, and the resulting immunoprecipitates were analyzed for phosphotyrosine by immunoblotting (4G10, *top*) or total β-catenin (*bottom*). *B*, cell layers were lysed in sample buffer. Lysates were electrophoresed, immunoblotted and analyzed for a phosphorylated form of β-catenin using an antibody that specifically recognizes β-catenin phosphorylated at tyrosine 654. Total β-catenin was used as a loading control. *C* and *D*, HMVECs were pretreated with NAC (*C*) or DPI (*D*) before treatment with 10 ng/ml VEGF, and the phosphorylation of β-catenin was monitored by Western blotting.

VEGF treatment reduced the association between VE-cadherin and p120-catenin (Fig. 5*D*). However, expression of the Y658F mutant or the double mutant attenuated the VEGF-induced VE-cadherin/p120-catenin dissociation. Similar results were seen when the VE-cadherin/β-catenin complex was examined. Again, in cells expressing WT VE-cadherin VEGF treatment caused a reduction in the amount of β-catenin that was complexed with VE-cadherin (Fig. 5*E*). However, in cells expressing the Y731F or the double mutant

VEGF was unable to induce VE-cadherin/β-catenin dissociation. Collectively, these results suggest that the regulation of microvascular permeability by VEGF requires, in part, the phosphorylation of VE-cadherin at tyrosines 658 and 731.

To further examine the integrity of the adherens junction, a coimmunoprecipitation analysis was performed to look at the extent of interaction between endogenous VE-cadherin and β-catenin. As demonstrated in Fig. 6*A*, VE-cadherin and β-catenin strongly co-immunoprecipitate under control conditions. However, upon treatment with VEGF there was a reduction in the amount of β-catenin that co-immunoprecipitated with VE-cadherin, suggesting that VEGF treatment decreases the interaction between VE-cadherin and β-catenin. Treatment with NAC prevented the dissociation of β-catenin with VE-cadherin, suggesting that ROS are necessary for the disruption of this interaction. In addition to the interaction between VE-cadherin and β-catenin we also examined the interaction between VE-cadherin and p120-catenin. We found that, under control conditions VE-cadherin and p120-catenin co-immunoprecipitate (Fig. 6*B*). However, upon treatment with VEGF there is a reduction in the amount of p120 catenin that co-immunoprecipitated with VE-cadherin. Treatment with NAC prevented the VEGF-induced dissociation of VE-cadherin and p120-catenin, suggesting that ROS are also necessary for the disruption of this interaction. Taken together, these data suggest that VEGF-induced ROS production regulates the tyrosine phosphorylation of adherens junction proteins VE-cadherin, β-catenin, and p120-catenin and their association.

Previous work has demonstrated that VEGF causes the activation of Rac1 in endothelial cells (28, 29). To confirm these observations, Rac1 GTP loading was measured by pulldown assays with glutathione *S*-transferase-p21-activating kinase. Indeed, we found that VEGF treatment caused a rapid activation of Rac1 (Fig. 7*A*). As we had demonstrated that ROS were required for the increase in VEGF-induced permeability (Fig.

A

B

C

D

E
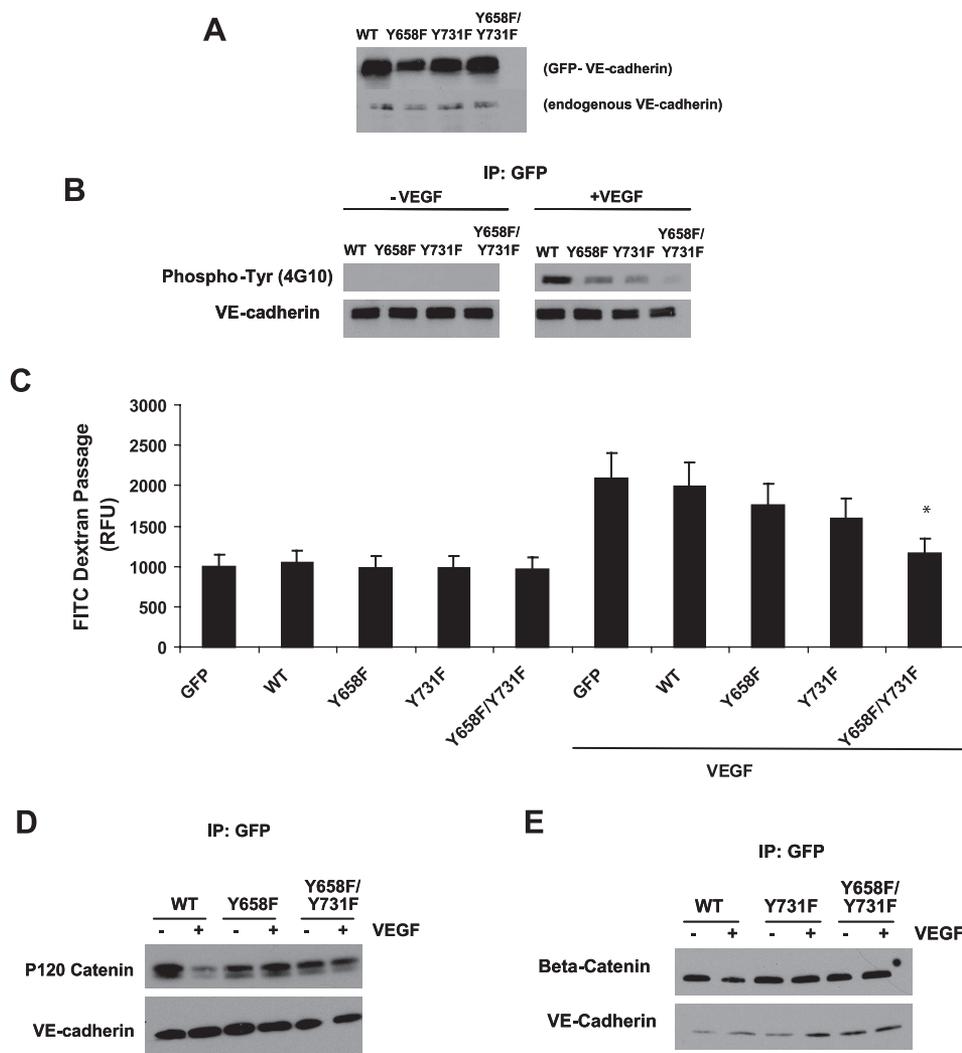
FIGURE 5. **VE-cadherin mutation dampens VEGF-induced permeability.** HMVECs were infected with adenovirus containing, WT VE-cadherin, or mutant VE-cadherins Y658F, Y731F, or Y658F/Y731F. *A*, cells were lysed and lysates were analyzed for the expression of both GFP-VE-cadherin and endogenous VE-cadherin by Western blot. *B*, cells were treated with 10 ng/ml VEGF for 15 min and lysed. GFP was immunoprecipitated from cell lysates using a mouse anti-GFP antibody, and the resulting immunoprecipitates were analyzed for phosphotyrosine by immunoblotting (4G10, *top*) or total VE-cadherin (*bottom*). *C*, cells were seeded in the upper well of a Transwell chamber and allowed to grow to confluence. 1 mg/ml FITC-dextran (M_r 10,000) was placed in the upper well, and cells were treated with 10 ng/ml VEGF for 30 min. A sample of medium from the lower chamber was then taken and the amount of FITC-dextran in the lower chamber was measured in a plate reader. *D*, cells were treated with 10 ng/ml VEGF for 15 min. GFP was immunoprecipitated from cell lysates, and immunoprecipitates were blotted for the presence of p120-catenin (*top*) and VE-cadherin (*bottom*). *E*, cells were treated with 10 ng/ml VEGF for 15 min. GFP was immunoprecipitated from cell lysates, and immunoprecipitates were blotted for the presence of β-catenin (*top*) and VE-cadherin (*bottom*). *, $p < 0.05$ Student's *t* test.

resulted in an increase in ROS production. However, in cells where Rac expression had been knocked down the ability of VEGF to induce ROS was greatly attenuated (Fig. 8*B*).

Once we had demonstrated that Rac was required for VEGF-induced ROS formation we asked whether Rac might also be required for VEGF-induced VE-cadherin phosphorylation, because we had already shown this to be ROS-dependent. RNA interference was again used to knock down Rac1 expression, and the ability of VEGF to induce phosphorylation of VE-cadherin at the catenin binding sites (Tyr-658 and Tyr-731) was monitored. We observed that cells transfected with Rac1 siRNA show a severe attenuation in the VEGF-induced VE-cadherin phosphorylation, as compared with the cells transfected with a non-targeting siRNA (Fig. 9).

Finally, we sought to determine whether Rac was also required for the VEGF-mediated increase in microvascular permeability. As shown in Fig. 10, cells transfected with a non-targeting siRNA are able to enhance vascular permeability upon VEGF treatment. However, knockdown of Rac1 abrogates the VEGF-induced permeability effect. Taken together our data demonstrate that Rac1 activation is necessary for VEGF-mediated vascular permeability and that the activation of Rac is required upstream of ROS generation in this pathway.

DISCUSSION

VEGF has a well known and well studied role in angiogenesis. However, the molecular mechanisms that regulate VEGF-induced permeability in the microvasculature, the first described function of VEGF, remain incompletely understood (4, 5). Recent studies have sought to determine the pathways through which VEGF regulates vascular permeability; however, these studies have focused primarily on HUVECs, endothelial cells from large vessels and not on cells of the microvasculature. Because the microvasculature represents the vessels where the largest changes in permeability occur and because VEGF is known to greatly alter microvascular permeability, the focus of this study was to determine the mechanism through which VEGF regulates microvascular permeability. We found that VEGF regulates microvas-

2), we wondered whether ROS might also be required for the VEGF-induced activation of Rac. To determine this we treated cells with NAC before VEGF treatment and then performed a PAK-binding domain pulldown assay to analyze the levels of active Rac. We found that scavenging ROS with NAC had no effect on the ability of VEGF to activate Rac (Fig. 7*B*). Once we had determined that ROS were not required for Rac activation we wondered if the inverse might be true. Was Rac required for ROS production in response to VEGF treatment? To answer this question we used RNA interference to knock down Rac1 expression in HMVECs (Fig. 8*A*), and the ability of VEGF to induce ROS formation was measured. We observed that under control non-targeting siRNA conditions VEGF treatment

cular permeability through the activation of Rac1 and the production of ROS. These molecules, in turn, regulate the tyrosine phosphorylation of adherens junction proteins VE-cadherin and β-catenin, ultimately regulating junctional integrity.

Until recently, ROS production in non-phagocytic cells has been viewed primarily as a harmful byproduct of various metabolic activities that cause DNA damage and lead to the oxidation of membrane proteins and lipids. In phagocytic cells there is a Rac-activated NADPH oxidase that generates ROS (30). However, the identification of a Rac-regulated NADPH oxidase in non-phagocytic cells raised the possibility

that ROS served other functions (31). Numerous studies have shown that ROS increase permeability both *in vitro* and *in vivo* (32, 33). Our results show that VEGF leads to ROS production in the microvasculature and that these ROS are required for the increase in permeability observed in response to VEGF treatment. Consistent with our results, earlier work has demonstrated that VEGF will increase superoxide production in endothelial cells of larger vessels and that this is required for the angiogenic phenotype (34). Furthermore, growth factors, including platelet-derived growth factor and EGF stimulate the generation of ROS (21, 35). In ischemia reperfusion injury, the generation of ROS derives from both the endothelium as well as from activated leukocytes, and the associated increase in permeability has been shown to be inhibited by antioxidants and free radical scavengers (32). Likewise, we demonstrate that the VEGF-induced vascular permeability is also attenuated by NAC, a free radical scavenger, and DPI, a flavoprotein inhibitor. These studies contribute to the increasing recognition that ROS have a role in signal transduction pathways that regulate diverse cellular responses, including migration, growth, and differentiation (36).

NADPH oxidase is a major source of ROS production in endothelial cells (25), and Rac1 is a critical component of endothelial NADPH oxidase (25, 37). Appropriate levels of active Rac are required for the formation and maintenance of adher-
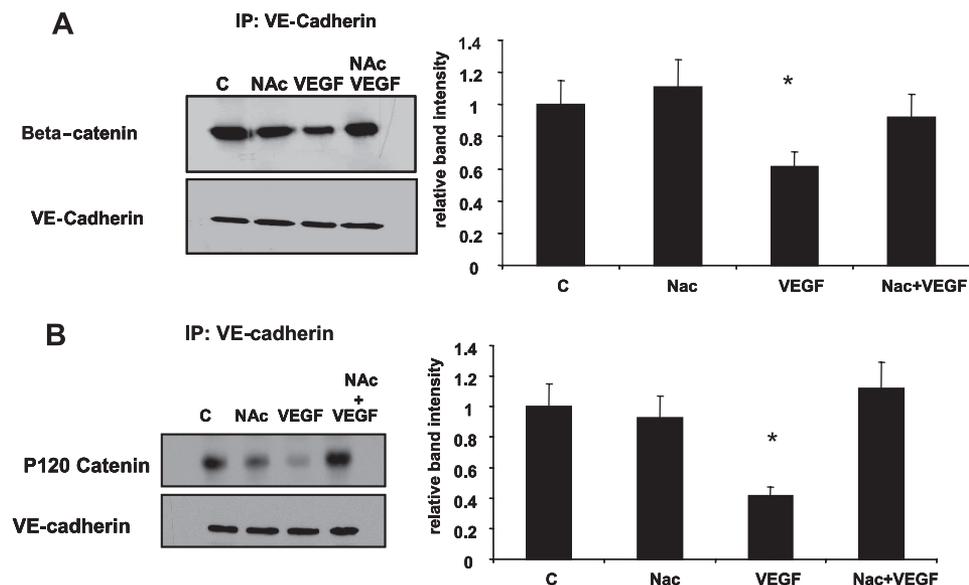
FIGURE 6. **VEGF treatment causes the ROS-dependent dissociation of VE-cadherin and β-catenin and VE-cadherin and p120-catenin.** HMVECs were pretreated with NAC for 2 h before treatment with 10 ng/ml VEGF for 15 min. VE-cadherin was immunoprecipitated from cell lysates, and immunoprecipitates were blotted for the presence of β-catenin (A) and p120-catenin (B).
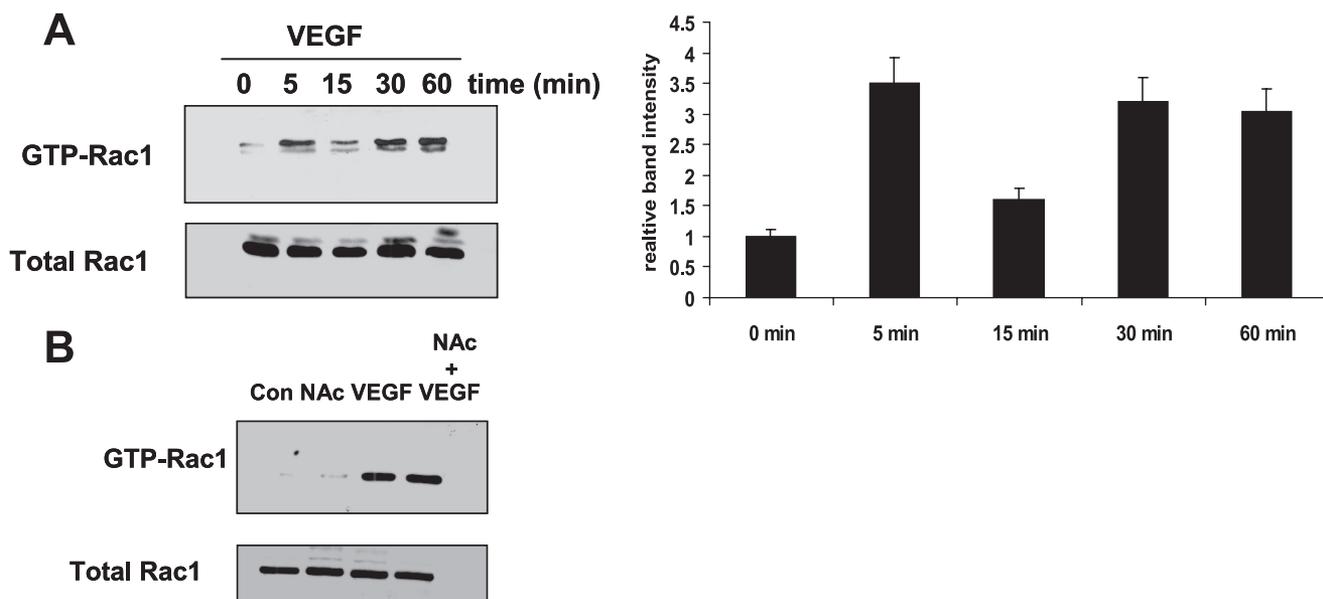
FIGURE 7. **VEGF treatment leads to the activation of Rac.** A, HMVECs were treated with 10 ng/ml VEGF for increasing time, and the activation of Rac was measured through a GST-PAK-binding domain pulldown assay as described under "Experimental Procedures." B, HMVECs were pretreated with NAC before treatment with VEGF. The activation of Rac was measured through a GST-PAK-binding domain pulldown assay.

A

B
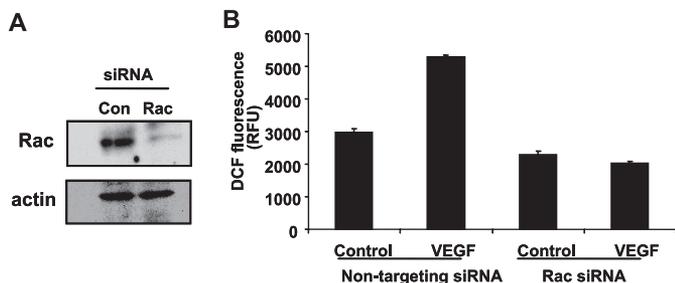
FIGURE 8. **Rac is required for VEGF-induced ROS generation.** *A*, HMVECs were transfected with Rac siRNA or non-targeting siRNA for 72 h. Cells were then lysed in sample buffer, electrophoresed, and immunoblotted with an antibody against Rac1 or actin. *B*, HMVECs were transfected with Rac siRNA or a non-targeting siRNA for 72 h. Cells were then treated with10 ng/ml VEGF and ROS generation was monitored by DCF fluorescence.
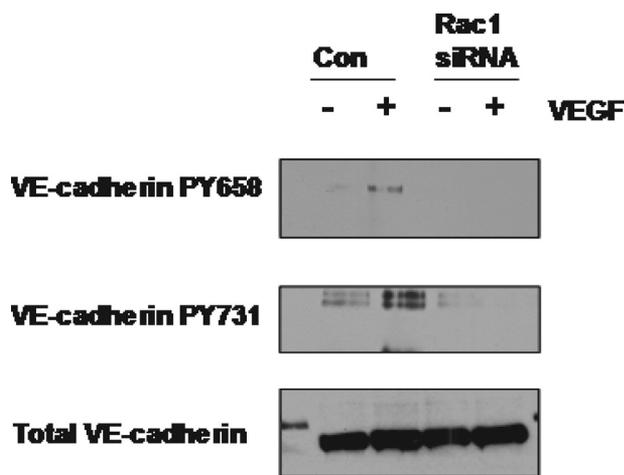
FIGURE 9. **Rac is required for VEGF-induced VE-cadherin phosphorylation.** HMVECs were transfected with Rac siRNA or non-targeting for 72 h. Cells were then treated with 10 ng/ml VEGF. Cells were lysed in sample buffer, and lysates were electrophoresed and immunoblotted with antibodies against VE-cadherin phosphorylated at Tyr-658 and Tyr-731. Total VE-cadherin was used as a loading control.
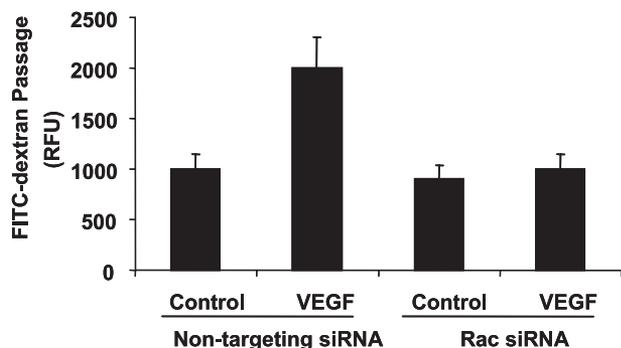
FIGURE 10. **Rac is required for VEGF-induced permeability.** HMVECs were transfected with Rac siRNA or non-targeting for 72 h. Cells were seeded in the upper well of a Transwell chamber and allowed to grow to confluence. 1 mg/ml FITC-dextran (M_r 10,000) was placed in the upper well, and cells were treated with 10 ng/ml VEGF for 30 min. A sample of medium from the lower chamber was then taken, and the amount of FITC-dextran in the lower chamber was measured in a plate reader.

ens junctions and either too high or too low activities promote disassembly. Both constitutively active and dominant negative Rac increase endothelial permeability, consistent with the level of Rac needing to be finely tuned for optimal junctional integrity (38). In addition, several groups have demonstrated that activation of Rac1 in response to sphigosine 1-phosphate

enhances barrier function of endothelial monolayers (39, 40). However, we and others have shown that activation of Rac1 downstream of VEGF, and other growth factors, promotes junction disassembly and increase permeability (18, 41–43). In addition, VEGF has been observed to regulate endothelial cell permeability through PAK, a direct downstream effector of Rac (44). It seems that it is more complex than simply high Rac activation leading to increased permeability. That active Rac can both increase and decrease permeability depending on the stimulus leads us to suggest that the route of activation may be critical and that different scaffolding proteins may direct Rac signaling pathways in different directions.

Tyrosine phosphorylation of adherens junction proteins has long been associated with the disassembly of cell-cell adhesions, although the precise mechanism has not been resolved (26, 27, 45). Several proteins, including cadherins and catenins, become prominently tyrosine-phosphorylated when PTPs are inhibited or when tyrosine kinases are activated. A number of PTPs, including VE-PTP, PTPμ, and SHP-2, can influence VE-cadherin function by altering its tyrosine phosphorylation state (46–49). VEGF treatment can disrupt the association between VE-cadherin and VE-PTP resulting in enhanced tyrosine phosphorylation of VE-cadherin and decreased barrier function (50). ROS oxidize a critical cysteine residue in the catalytic site of tyrosine phosphatases, thereby deactivating these enzymes, resulting in increased tyrosine phosphorylation (51). VEGF treatment also induces Src activation, which leads to the tyrosine phosphorylation of several junctional proteins (52, 53). Additional work has demonstrated that Src inhibition or deficiency results in defective VEGF-induced vascular permeability due to the stabilization of VE-cadherin in endothelial cell junctions (52, 54). Within the endothelium, elevated tyrosine phosphorylation is associated with a decrease in barrier function (55–58). Our data demonstrate that VEGF treatment leads to the tyrosine phosphorylation of VE-cadherin on at least two sites that lie within the β-catenin and p120 catenin binding regions. Additionally, we show that VEGF treatment results in β-catenin phosphorylation itself. The tyrosine phosphorylation of VE-cadherin at Tyr-731 has been reported to cause a loss in the ability of VE-cadherin to bind β-catenin (17). Additionally, tyrosine phosphorylation of β-catenin has also been reported to decrease its affinity for the cadherin and increase its turnover at junctions (59, 60). Although the enhanced phosphorylation of VE-cadherin at Tyr-731 changes the binding affinity for β-catenin and likely decreases cytoskeletal attachment, the phosphorylation at Tyr-658 decreases the affinity of VE-cadherin for p120 catenin (17). It has been demonstrated that the binding of p120 to VE-cadherin prevents VE-cadherin internalization thereby acting to stabilize the junction (61). The tyrosine phosphorylation of VE-cadherin at these catenin binding sites suggests that VEGF may be regulating microvascular permeability through mechanisms controlling both cytoskeletal attachment and junctional stability.

Our data provide new insight into the molecular mechanisms by which VEGF regulates permeability of the microvasculature. In this work we have identified a pathway by which

VEGF-induced Permeability Requires Rac and ROS

VEGF increases endothelial permeability, demonstrating that VEGF leads to a Rac-mediated generation of ROS, which, in turn, elevates the tyrosine phosphorylation of several junctional proteins, including VE-cadherin and β-catenin. Rac activation and ROS generation have been implicated in many pathological situations where vascular permeability is altered. It will be interesting to determine whether these can also be attributed to the enhanced tyrosine phosphorylation of VE-cadherin and β-catenin.

REFERENCES

1. Dejana, E. (2004) *Nat. Rev. Mol. Cell Biol.* **5,** 261–270
2. Muller, W. A. (2003) *Trends Immunol.* **24,** 327–334
3. Vestweber, D. (2008) *Arterioscler. Thromb. Vasc. Biol.* **28,** 223–232
4. Senger, D. R., Asch, B. B., Smith, B. D., Perruzzi, C. A., and Dvorak, H. F. (1983) *Nature* **302,** 714–715
5. Senger, D. R., Perruzzi, C. A., Feder, J., and Dvorak, H. F. (1986) *Cancer Res.* **46,** 5629–5632
6. Connolly, D. T., Heuvelman, D. M., Nelson, R., Olander, J. V., Eppley, B. L., Delfino, J. J., Siegel, N. R., Leimgruber, R. M., and Feder, J. (1989) *J. Clin. Invest.* **84,** 1470–1478
7. Cross, M. J., Dixelius, J., Matsumoto, T., and Claesson-Welsh, L. (2003) *Trends Biochem. Sci.* **28,** 488–494
8. Gotsch, U., Borges, E., Bosse, R., Böggemeyer, E., Simon, M., Mossmann, H., and Vestweber, D. (1997) *J. Cell Sci.* **110,** 583–588
9. Corada, M., Mariotti, M., Thurston, G., Smith, K., Kunkel, R., Brockhaus, M., Lampugnani, M. G., Martin-Padura, I., Stoppacciaro, A., Ruco, L., McDonald, D. M., Ward, P. A., and Dejana, E. (1999) *Proc. Natl. Acad. Sci. U.S.A.* **96,** 9815–9820
10. Carmeliet, P., Lampugnani, M. G., Moons, L., Breviario, F., Compernolle, V., Bono, F., Balconi, G., Spagnuolo, R., Oostuyse, B., Dewerchin, M., Zanetti, A., Angellilo, A., Mattot, V., Nuyens, D., Lutgens, E., Clotman, F., de Ruiter, M. C., Gittenberger-de Groot, A., Poelmann, R., Lupu, F., Herbert, J. M., Collen, D., and Dejana, E. (1999) *Cell* **98,** 147–157
11. May, C., Doody, J. F., Abdullah, R., Balderes, P., Xu, X., Chen, C. P., Zhu, Z., Shapiro, L., Kussie, P., Hicklin, D. J., Liao, F., and Bohlen, P. (2005) *Blood* **105,** 4337–4344
12. Hordijk, P. L., Anthony, E., Mul, F. P., Rientsma, R., Oomen, L. C., and Roos, D. (1999) *J. Cell Sci.* **112,** 1915–1923
13. Crosby, C. V., Fleming, P. A., Argraves, W. S., Corada, M., Zanetta, L., Dejana, E., and Drake, C. J. (2005) *Blood* **105,** 2771–2776
14. Fukuhara, S., Sakurai, A., Sano, H., Yamagishi, A., Somekawa, S., Takakura, N., Saito, Y., Kangawa, K., and Mochizuki, N. (2005) *Mol. Cell Biol.* **25,** 136–146
15. Kooistra, M. R., Corada, M., Dejana, E., and Bos, J. L. (2005) *FEBS Lett.* **579,** 4966–4972
16. Ozawa, M., and Kemler, R. (1998) *J. Biol. Chem.* **273,** 6166–6170
17. Potter, M. D., Barbero, S., and Cheresh, D. A. (2005) *J. Biol. Chem.* **280,** 31906–31912
18. van Wetering, S., van Buul, J. D., Quik, S., Mul, F. P., Anthony, E. C., ten Klooster, J. P., Collard, J. G., and Hordijk, P. L. (2002) *J. Cell Sci.* **115,** 1837–1846
19. Abid, M. R., Kachra, Z., Spokes, K. C., and Aird, W. C. (2000) *FEBS Lett.* **486,** 252–256
20. Abid, M. R., Tsai, J. C., Spokes, K. C., Deshpande, S. S., Irani, K., and Aird, W. C. (2001) *FASEB J.* **15,** 2548–2550
21. Sundaresan, M., Yu, Z. X., Ferrans, V. J., Sulciner, D. J., Gutkind, J. S., Irani, K., Goldschmidt-Clermont, P. J., and Finkel, T. (1996) *Biochem. J.* **318,** 379–382
22. Yeh, L. H., Park, Y. J., Hansalia, R. J., Ahmed, I. S., Deshpande, S. S., Goldschmidt-Clermont, P. J., Irani, K., and Alevriadou, B. R. (1999) *Am. J. Physiol.* **276,** C838–C847
23. Sohn, H. Y., Keller, M., Gloe, T., Morawietz, H., Rueckschloss, U., and Pohl, U. (2000) *J. Biol. Chem.* **275,** 18745–18750
24. Allingham, M. J., van Buul, J. D., and Burridge, K. (2007) *J. Immunol.* **179,** 4053–4064
25. Babior, B. M. (2000) *IUBMB Life* **50,** 267–269
26. Volberg, T., Zick, Y., Dror, R., Sabanay, I., Gilon, C., Levitzki, A., and Geiger, B. (1992) *EMBO J.* **11,** 1733–1742
27. Birchmeier, W., and Behrens, J. (1994) *Biochim. Biophys. Acta* **1198,** 11–26
28. Zeng, H., Zhao, D., and Mukhopadhyay, D. (2002) *J. Biol. Chem.* **277,** 4003–4009
29. Garrett, T. A., Van Buul, J. D., and Burridge, K. (2007) *Exp. Cell Res.* **313,** 3285–3297
30. Bokoch, G. M., and Diebold, B. A. (2002) *Blood* **100,** 2692–2696
31. Irani, K., and Goldschmidt-Clermont, P. J. (1998) *Biochem. Pharmacol.* **55,** 1339–1346
32. Lum, H., and Roebuck, K. A. (2001) *Am. J. Physiol. Cell Physiol.* **280,** C719–C741
33. Mehta, D., and Malik, A. B. (2006) *Physiol. Rev.* **86,** 279–367
34. Ushio-Fukai, M., Tang, Y., Fukai, T., Dikalov, S. I., Ma, Y., Fujimoto, M., Quinn, M. T., Pagano, P. J., Johnson, C., and Alexander, R. W. (2002) *Circ. Res.* **91,** 1160–1167
35. Bae, Y. S., Kang, S. W., Seo, M. S., Baines, I. C., Tekle, E., Chock, P. B., and Rhee, S. G. (1997) *J. Biol. Chem.* **272,** 217–221
36. Li, A. E., Ito, H., Rovira, I. I., Kim, K. S., Takeda, K., Yu, Z. Y., Ferrans, V. J., and Finkel, T. (1999) *Circ. Res.* **85,** 304–310
37. Görlach, A., Brandes, R. P., Nguyen, K., Amidi, M., Dehghani, F., and Busse, R. (2000) *Circ. Res.* **87,** 26–32
38. Wójciak-Stothard, B., Potempa, S., Eichholtz, T., and Ridley, A. J. (2001) *J. Cell Sci.* **114,** 1343–1355
39. Garcia, J. G., Liu, F., Verin, A. D., Birukova, A., Dechert, M. A., Gerthoffer, W. T., Bamberg, J. R., and English, D. (2001) *J. Clin. Invest.* **108,** 689–701
40. Vouret-Craviari, V., Bourcier, C., Boulter, E., and van Obberghen-Schilling, E. (2002) *J. Cell Sci.* **115,** 2475–2484
41. Braga, V. M., Del Maschio, A., Machesky, L., and Dejana, E. (1999) *Mol. Biol. Cell* **10,** 9–22
42. van Wetering, S., van den Berk, N., van Buul, J. D., Mul, F. P., Lommerse, I., Mous, R., ten Klooster, J. P., Zwaginga, J. J., and Hordijk, P. L. (2003) *Am. J. Physiol. Cell Physiol.* **285,** C343–C352
43. Gavard, J., and Gutkind, J. S. (2006) *Nat. Cell Biol.* **8,** 1223–1234
44. Stockton, R. A., Schaefer, E., and Schwartz, M. A. (2004) *J. Biol. Chem.* **279,** 46621–46630
45. Volberg, T., Geiger, B., Dror, R., and Zick, Y. (1991) *Cell Regul.* **2,** 105–120
46. Nawroth, R., Poell, G., Ranft, A., Kloep, S., Samulowitz, U., Fachinger, G., Golding, M., Shima, D. T., Deutsch, U., and Vestweber, D. (2002) *EMBO J.* **21,** 4885–4895
47. Young, B. A., Sui, X., Kiser, T. D., Hyun, S. W., Wang, P., Sakarya, S., Angelini, D. J., Schaphorst, K. L., Hasday, J. D., Cross, A. S., Romer, L. H., Passaniti, A., and Goldblum, S. E. (2003) *Am. J. Physiol. Lung Cell Mol. Physiol.* **285,** L63–L75
48. Balsamo, J., Leung, T., Ernst, H., Zanin, M. K., Hoffman, S., and Lilien, J. (1996) *J. Cell Biol.* **134,** 801–813
49. Ukropec, J. A., Hollinger, M. K., Salva, S. M., and Woolkalis, M. J. (2000) *J. Biol. Chem.* **275,** 5983–5986
50. Nottebaum, A. F., Cagna, G., Winderlich, M., Gamp, A. C., Linnepe, R., Polaschegg, C., Filippova, K., Lyck, R., Engelhardt, B., Kamenyeva, O., Bixel, M. G., Butz, S., and Vestweber, D. (2008) *J. Exp. Med.* **205,** 2929–2945
51. Rhee, S. G., Bae, Y. S., Lee, S. R., and Kwon, J. (2000) *Sci. STKE 2000,* E1
52. Weis, S., Cui, J., Barnes, L., and Cheresh, D. (2004) *J. Cell Biol.* **167,** 223–229
53. Esser, S., Lampugnani, M. G., Corada, M., Dejana, E., and Risau, W. (1998) *J. Cell Sci.* **111,** 1853–1865
54. Weis, S., Shintani, S., Weber, A., Kirchmair, R., Wood, M., Cravens, A., McSharry, H., Iwakura, A., Yoon, Y. S., Himes, N., Burstein, D., Doukas, J., Soll, R., Losordo, D., and Cheresh, D. (2004) *J. Clin. Invest.* **113,** 885–894
55. Bogatcheva, N. V., Garcia, J. G., and Verin, A. D. (2002) *Vascul. Pharma-*

col. **39,** 201–212

56. Garcia, J. G., Schaphorst, K. L., Verin, A. D., Vepa, S., Patterson, C. E., and Natarajan, V. (2000) *J. Appl. Physiol.* **89,** 2333–2343

57. Sui, X. F., Kiser, T. D., Hyun, S. W., Angelini, D. J., Del Vecchio, R. L., Young, B. A., Hasday, J. D., Romer, L. H., Passaniti, A., Tonks, N. K., and Goldblum, S. E. (2005) *Am. J. Pathol.* **166,** 1247–1258

58. Young, B. A., Wang, P., and Goldblum, S. E. (1998) *Biochem. Biophys. Res. Commun.* **251,** 320–327

59. Huber, A. H., Stewart, D. B., Laurents, D. V., Nelson, W. J., and Weis, W. I. (2001) *J. Biol. Chem.* **276,** 12301–12309

60. Lilien, J., and Balsamo, J. (2005) *Curr. Opin. Cell Biol.* **17,** 459–465

61. Xiao, K., Garner, J., Buckley, K. M., Vincent, P. A., Chiasson, C. M., Dejana, E., Faundez, V., and Kowalczyk, A. P. (2005) *Mol. Biol. Cell* **16,** 5141–5151

62. Sander, E. E., van Delft, S., ten Klooster, J. P., Reid, T., van der Kammen, R. A., Michiels, F., and Collard, J. G. (1998) *J. Cell. Biol.* **143,** 1385–1398